附件：

论 文 写 作 要 求

1 中文论文篇幅不超过 8 页左右，每页 44 行×44 字(含图表、标点符号、空格及英文摘要)。

2 论文题目不超过 20 字，题目中不宜使用非公知的缩略词、首字母缩写字符、代号等。

3 摘要要求：

（1）必须对论文进行认真的主题分析，根据论文的主题概念组织好文摘内容，应包括研究的问题和目的、过程和方法、结果和结论。不说无用的话，不能与引言和结论简单重复。

（2）具有独立性和自含性，不用图表、化学结构式和非公知公认的符号或术语；不宜引用图、表、公式和参考文献的序号；对于那些仅为同行所熟悉的缩略语，应在题目、文摘中至少出现一次全称。

（3）篇幅：中文摘要 300 字左右，英文摘要 100～150 words，文摘第一句应避免与题目（title）重复。

（4）采用第三人称，不用 “作者、笔者、我们” “本文（This paper）”. 尽量不要使用 not only…but also 用 and 就行了；用过去时态叙述作者工作，用现在时态叙述作者结论；可数名词尽量用复数；可直接用名词或名词短语作定语的情况下，要少用 of 句型；少用“It is reported that”；尽量不用长句、复合句，而应使用简明、直接的短句形式。

摘要例 1：研究了亚共晶成分的铝硅合金中铁相形态与熔体处理的关系，发现六氯乙烷精炼强烈促进初生α铁相的产生。在未经精炼处理时，合金微观组织中的铁相基本呈发达的树枝状，只有少量为初生汉字状铁相。用六氯乙烷精炼后，合金的组织中开始出现大量六角形的初生相。这种六角形铁相的形貌受冷却速度的影响较大。在精炼以后对合金长时间保温对该六角形铁相的出现和形态没有影响。由六氯乙烷精炼导致合金中大量六角形初生α铁相出现，可能是六氯乙烷精炼提高了α铁相的形核温度。

摘要例 2：通过参数变换，将混沌系统的适当参数作为摄动小参数，从而将 Lorenz 系统、Chen 系统和 Lü系统看作快慢型自治系统，利用几何奇异摄动理论对其动力学行为进行分析。由退化快子系统得到零阶慢流形的表达式，利用 Fenichel 保持定理得出慢流形的存在性，慢流形与零阶慢流形是充分接近的。将慢流形的表达式展开为摄动参数的渐进级数，得到三个快慢型系统的慢流形的方程，它们都近似于平面。基于慢流形对三个系统的平衡点和轨线作定性分析，平衡点全在慢流形上，慢轨线与慢流形是充分接近的。

摘要例3：为了实现具有较大阻抗的圆形槽波导与阻抗较小的有源器件之间的阻抗匹配，在W波段圆形槽波导振荡器中采用了径向盘结构，通过改变径向盘的厚度来调节输入阻抗的大小。用完全匹配层将圆形槽波导的开放边界截断为有限区域后，应用有限元法分析基于圆形槽波导的毫米波元件。为了避免传统的有限元方法所遇到的伪模式问题，选用了棱边元对圆形槽振荡器中的径向盘结构的输入阻抗进行数值计算。得出了频率在85～100GHz之间，对应于不同的径向盘厚度的输入阻抗。径向盘的厚度小于0.13mm时输入阻抗较小。计算结果为用于W 波段圆形槽波导振荡器的径向盘的优化设计提供了依据。

摘要例 4: In order to match the widely different impedances between circular groove guide and millimeter wave semi-conductor device, the radial disk structure is used in W 2band oscillator based on circular groove guide. By varying the radial disk thickness, the input impedance can be changed. Perfectly matched layer (PML) is app lied to truncate the open boundary of circular groove guide to fulfill the requirement of limited domain that the finite element method (FEM) can proceed. The in-put impedance from 85 to 100 GHz was calculated by tetrahedral edge element to eliminate spurious

*Corresponding author (email: suijun@mail.etp.ac.cn)

solutions. When thickness is less than 0.13 mm, the input impedance of the radial mount is relatively low. The numerical results that the impedance changes with the disk thickness are very useful for design and adjustment of W 2b and circular groove guide oscillators.

4　引言介绍研究背景、研究现状，指出现有研究的优点和不足之处，然后引到自己的研究上来。见范例：

引言示例 1：液压式固有频率可控动力消振器

动力消振器是一个附加于主振系上的由质量和弹簧组成的振动系统。当其固有频率与主振系的振动频率相等时，主振系便不发生振动[1]。由于动力消振器具有良好的消振效果，自本世纪初发明以来已得到广泛应用。（*介绍研究对象及其基本特征*）但传统动力消振器的缺点在于其固有频率固定不变，不能在使用过程中加以调整，更不能随主振系振动频率的变化对它进行控制，，因而它只适用于消除基频基本不变的振动。对于更为常见的频率经常改变的振动系统，它不能收到良好的消振效果，甚至导致更大危害[2]。（*说明前人研究的不足和存在的问题，亦阐明了研究理由和背景*）

笔者提出一种可用于消除变频振动的新方法，即采用液压式固有频率可控动力消振器来跟踪振动频率变化，使之在变频条件下达到良好的消振效果。（*引出作者的研究方案*）

引言示例 2：语音情感特征提取与识别的实现

语音的情感识别是目前信号处理及模式识别领域的一个新的研究热点，其任务是利用计算机从给定的语音中准确提取情感特征，并根据这些情感特征确定被测对象的情感状态。该研究在信号处理、心理学研究、机器人技术、虚拟现实技术、人工智能以及新型人机交互技术等许多领域有着重要的应用价值。（*介绍研究对象及其研究特征、意义*）

典型的语音情感识别系统主要包括情感特征的提取及分类识别，其中情感特征提取的好坏直接影响情感状态识别的正确率，优秀的情感特征提取算法应能实时、有效地提取反映情感状态的特征，同时对于不同语言背景的变化有一定的鲁棒性。目前已有一些学者对语音情感识别问题进行了研究[1-4]，但识别率和可用性都有待进一步提高。（*研究的目标和目前的不足*）为此，利用汉明窗提取语音信号中情感特征参数，采用贡献分析法计算出情感特征参数权值，应用加权欧氏距离模板匹配法识别语音情感，最后通过原型系统测试验证该方法有效性。（*引出作者的研究方案*）

引言示例 3：基于时域声辐射模态的结构噪声主动控制

自上世纪九十年代学者们提出了声辐射模态概念以来，国内外众多学者，在不同的角度进行了大量的研究[1-3]。声辐射模态是振动辐射体的固有属性，反映了辐射体的辐射性质，利用声辐射模态来研究外部声辐射问题的优点在于消除了结构模态中复杂的耦合项，使得计算和控制声辐射更为简单。初步的研究成果，已显示出它在结构噪声主动控制中的应用潜力[4-5]。（*研究对象及背景、意义介绍*）但迄今为止对声辐射模态的研究大都集中在频域里进行，在时域里对声辐射模态的研究还少有报道。作者在时域里对辐射模态进行研究，以从另一个的角度扩大声辐射模态的应用范围。（*研究目标的引出*）

5　图题、表题要简洁；图以 6 幅为限，表格采用“三线表”。灰度图、照片图及复杂的图应提供 JPG 格式的原件。许多作者不注

意保留图片的原始底样，待稿件录用时只是将原电子稿 word 文件中图片复制提取出来，这种图片的分辨率远不能满足要求。因此要将最初生成的每一张图片单独保存为一个 JPG 文件以备用。

6　确定中图分类号；标注文献标识码(其选择见表 1)、文章编号(由编辑部填写)、第一、二作者简介及研究方向。

7　论文中的变量、函数及英文符号应统一、规范、不重复，不宜采用非公认的缩略词。公式、算式及语言中的变量、英文符号等应注意大小写、黑白、正斜体区分，必要时应另外向编辑部单独文字说明。仔细检查以上内容避免出现计算机误操作和其他笔误。

8　关键词 5～8 个，“研究对象”放在第一位置。尽量从汉语主题词表中选取。

9　若论文与省、部级以上基金项目有关，均应标注项目名称及编号。

10　参考文献 10 篇以上，其中 80%应为期刊论文或会议论文，80%以上为近 5 年出版的文献，50%以上为外文文献。

11　参考文献必须在文中全部引用，引用次序需与所列参考文献的排列顺序一致。标准格式如下：

12．1　期刊(中文期刊须中英文对照)——著者．题名［J］．期刊名称(外文刊名可缩写、并省略缩写点)，出版年，卷号(期号)：起止页码．　(in Chinese)

例 1：冯玉才，冯剑琳．关联规则的增量式更新算法[J]．软件学报，2003，9(4)：301-306.

FENG Yu-cai, FENG Jian-lin.Incremental updating algorithms for mining association rules[J].*Journal of Software*, 2003, 9(4)： 301-306. (in Chinese)

12．2　书籍——著者．书名[M]．版次(第 1 版不注明)，译者.出版地：出版者，出版年：起止页码.

例 2：竺可桢．物候学[M]．北京：科学出版社，2001：234-238.

例 3：Timoshenko. *Theory of Plate and Shells*[M]．　NewYork：MeGrawHill，2000：156-168.

例 4：尼科里斯，普利高津．探索复杂性[M]．罗久里译．成都：四川教育出版社，2002：88-96.

12．3　论文集——著者．论文题名[C]//编者．文集名．出版地：出版者，出版年：起止页码.

例 5：张全福．理工科学报编辑工作[C]//郑福寿．学报编辑论丛．南京：河海大学出版社，2000：170-175.

例 6：Davidovits J. Geopolymer chemisty and properties[C]//*Proceedings of the First European Conference on Soft Mineralogy*. France：Parisian， 1998：132-136.

12．4　学位论文——作者．题名[D]．保存地点：保存单位，年份.

例 7：张笔生．微分半动力系统的不变集[D]．北京：北京大学数学系，2001.

12．5　专利——专利申请者．题名：专利国别，专利号[P].公告日期或公开日期.

例 8：朱银昌，赵不贿．一种直交变流三相微特电机：中国，ZL94244844．8[P]．1996-08-10.

12．6　电子文献——作者.题名[类别].文献引用地址，发表或更新日期/引用日期(任选)

类别代码：[DB/OL]网络数据库，[M/CD] 光盘图书，[J/OL] 网上期刊，[EB/OL] 电子公告

例 9：王明亮.中国标准化数据库系统工程进展[EB/OL].http://www.cajcd.edu.cn/pub/wml/980810-2.html,2004-08-14/2004-10-09.

12．7　参考文献中的文献类型标识［］的选择见下表。

专　著	论　文　集	报纸文章	期刊文章	学位论文	报　告	标　准	专　利
M	C	N	J	D	R	S	P

12．8　文献作者 3 名以内全部列出，4 名以上只列前 3 名，后加“，等”或“，et al”。外文作者姓前名后，名用缩写，不加缩

写点。中国作者的名字不能缩写，如 Zheng Guangmei 不能写成 Zheng G M。

表 1　各类文献标识码规范设置表

理论与应用研究论文	实用性成果学习实践总结	业务指导管理类文章	一般动态性信息	文件、资料
A	B	C	D	E

中文论文格式示例：

基于 HLA 的……建模

※※※[1, 2]，※※※[1]，※※※[1]
（1.重庆大学 计算机学院，重庆 400030； 2. 南京邮电大学 计算机学院，江苏 南京 210003）

摘要：为实现 DEVS 在智能建模与分布仿真能力方面的扩充，研究了基于 HLA 的 Agent-DEVS 协同仿真建模方法。以并行 DEVS 为基础，提出了 Agent-DEVS 联邦模型的形式化描述；将 Agent-DEVS 模型端口转换为 HLA 数据对象，确定了 Agent-DEVS 联邦模型结构，并分析了通信机制，分别建立了 Agent-DEVS 的知识更新与 HLA 的属性更新间的映射，以及 Agent-DEVS 的模型耦合与 HLA 的实例交互间的映射；最后结合抢险救灾物资保障的仿真建模进行了应用。结果表明，HLA 体系框架增强了 Agent-DEVS 模型的可重用性；知识更新机制丰富了 Agent-DEVS 模型的互操作性；同时，Agent-DEVS 模型的自治性与独立事务处理能力得到了进一步提高。

说明：摘要结构为：文章的目的，或针对问题（即"为了……"或"针对……问题"；是具体而非笼统的问题）；主要思想概述；主要工作概述；（注：以上 2 部分，也可只有主要工作概述）结论概述。英文摘要：采用被动语态；所做工作使用过去时；结论使用现在时。

关键词：仿真建模；离散事件仿真；智能体；可重用性；互操作性

说明：关键词 5-8 个，"研究对象"放在第一位置。从 Ei 数据库的主题词表 Thesaurus 中选取。

中图分类号：TP391.9　文献标志码：A　文章编号：

Collaborative modeling …· based on HLA

※※※[1, 2]，※※※[1]，※※※[1]
(1. College of Computer Science, Chongqing University, Chongqing 400030, China; 2. School of Computer Science and Technology, Nanjing University of Posts and Telecommunications, Nanjing，Jiangsu 210003，China)

说明：中文人名写法为 Luo Guanzhong

Abstract: In order to ….
Key words: simulation modeling; discrete event simulation; agents; reusability; interoperability

DEVS（即 discrete event system specification）是针对离散事件系统的形式化描述体系，它将每个子系统看作一个具有内部独立结构和输入输出接口的模块，这些模块通过连接关系组合成为更大的模块，从而形成规范化、层次化、模块化的描述[1]。但是，DEVS 对于模块内部的智能行为，以及模块间的协作问题，并没有提供直接的描述方法，而且随着模块数量的增长，交互问题成为瓶颈，需要进一步实现分布式协同仿真。在智能建模方面，曹琦等运用 Agent 建模思想对 DEVS 规范进行了扩展，得到了一种具备智能性和协作性描述能力的离散事件系统规范 Agent-DEVS[2]。在分布仿真方面，HLA（即 high level architecture）是标准的高层体系框架，它定义了构成各分布式仿真成员的功能和相互关系[3]。近年来，国内外就 DEVS 与 HLA 的结合

*Corresponding author (email: suijun@mail.etp.ac.cn)

问题展开了相关研究，以实现 DEVS 建模优势与 HLA 分布仿真能力的有机统一，如 Zacharewicz G 等在提出 GDEVS（即 generalized DEVS）规范的基础上，实现了 GDEVS/HLA 的分布式仿真环境[4]；Ounnar F 等为扁平协同式组织中的自主控制实体建立了 DEVS 模型，并将其集成到 HLA 分布式仿真环境中[5]；Sung C H 等利用 HLA 建立了一个混合仿真框架，以实现工程级模型（由 MATLAB/Simulink 创建）与事务级模型（由 DEVS 创建）间的互操作[6]；郭斌等提出了一种基于 HLA/DEVS 的协同仿真高层建模方法[7]。但是，这些研究在实现 DEVS 分布式仿真的同时，并没有解决智能建模的问题。

文中拟以具有智能描述能力的 Agent-DEVS 为基础，将其与 HLA 相结合，提出 Agent-DEVS 联邦模型的形式化描述，确定模型结构，分析通信机制，从而实现 DEVS 在智能建模与分布仿真能力方面的扩充，最后给出在抢险救灾物资保障中的应用实例。

说明：引言最后一段为文章工作框架。

1　Agent-DEVS 联邦模型的形式化描述

（正文略）

说明：表格采用三线表。曲线、图形、照片等，采用高质量、彩色图像。引言开始，排双栏。

4　结 论　　**说明：建议结论条理化叙述。**

（1）※※※。

（2）※※※。

（3）※※※。

参考文献（References）

[1] Zeigler B P, Praehofer H, Kim T G. *Theory of Modeling and Simulation: Integrating Discrete Event and Continuous Complex Dynamic Systems*[M]. 2en ed. San Diego: Academic Press, 2000.

[2] Cao Qi, He Zhongshi, Yu Lei. Agent-DEVS: an extended DEVS formalism for intelligent modeling and simulation[C]//*Proceedings of the Second International Conference on Modelling and Simulation*. Liverpool: World Academic Union, 2009: 286-291.

[3] Topçu O, Adak M, O?uztüzün H. A metamodel for federation architectures[J]. *ACM Transactions on Modeling and Computer Simulation*, 2008, 18(3): 25-53.

[4] Zacharewicz G, Frydman C, Giambiasi N. Mapping PIOVRA in GDEVS/HLA environment[C]//*Proceedings of the 2007 Summer Computer Simulation Conference*. San Diego: Society for Computer Simulation International, 2007: 1086-1093.

[5]Ounnar F, Pujo P, Mekaouche L, et al. Integration of a flat holonic form in an HLA environment[J]. *Journal of Intelligent Manufacturing*, 2009, 20(1): 91-111.

[6] Sung C H, Hong J H, Kim T G. Interoperation of DEVS models and differential equation models using HLA/RTI: hybrid simulation of engineering and engagement level models[C]//*Proceedings of the 2009 Spring Simulation Multiconference*. San Diego: Society for Computer Simulation International, 2009: 387-392.

[7] 郭 斌, 范文慧, 熊光楞. 基于 HLA/DEVS 的协同仿真高层建模研究[J]. 系统仿真学报, 2006, 18(8): 2174-2178.

Guo Bin, Fan Wenhui, Xiong Guangleng. Research of HLA/DEVS-based high level modeling for collaborative simulation[J]. *Journal of System Simulation*, 2006, 18(8): 2174-2178. (in Chinese)

[8]孙国兵, 杨 明, 刘 飞. 基于元模型的战场环境多分辨率建模[J]. 江苏大学学报：自然科学版, 2008, 29(4): 339-343.

Sun Guobing, Yang Ming, Liu Fei. Multi-resolution modeling of battlefield environment based on meta-model[J]. *Journal of Jiangsu University: Natural Science Edition*, 2008, 29(4): 339-343. (in Chinese)

[9] 曹 琦, 何中市, 黄永文, 等. 基于HLA/MAS的野营保障仿真建模研究[J]. 系统仿真学报, 2009, 21(5): 1474-1478.

Cao Qi, He Zhongshi, Huang Yongwen, et al. Research on simulation and modeling of camping

service based on HLA/MAS[J]. *Journal of System Simulation*, 2009, 21(5): 1474-1478. (in Chinese)
[10] Lee J K, Lee M W, Chi S D. DEVS/HLA-based modeling and simulation for intelligent transportation systems[J]. *Simulation*, 2003, 79(8): 423-439.

收稿日期: 2010-01-11 **说明：这 3 项内容，用脚注放于首页下方。作者简介的 7 项内容要全。**
基金项目: ※※※市自然科学基金资助项目(※※※); 国防科研计划项目(※※※)
作者简介: ※※※(1976—), 男, 重庆人, 博士研究生(※※※@163.com), 主要从事系统建模与仿真研究. ※※※(1965—), 男, 四川成都人, 教授, 博士生导师(※※※@cqu.edu.cn), 主要从事计算机软件与理论研究.

英文论文格式如下：

Experimental investigation on a parabolic trough solar collector for thermal power generation

LIU QiBin[1], WANG YaLong[1,2], GAO ZhiChao[1,2], SUI Jun[1*], JIN HongGuang[1] & LI HePing[3]

[1] *Institute of Engineering Thermophysics, Chinese Academy of Sciences, Beijing 100190, China;*
[2] *Graduate University of Chinese Academy of Sciences, Beijing 100049, China;*
[3] *China Huadian Engineering Co., Ltd, Beijing 100044, China*

Received ; accepted

Developing solar thermal power technology in an effective manner is a great challenge in China. In this paper an experiment platform of a parabolic trough solar collector system (PTCS) was developed for thermal power generation, and the performance of the PTCS was experimentally investigated with synthetic oil as the circulate heat transfer fluid (HTF). The solar collector's efficiency with the variation of the solar flux and the flow rate of the HTF was identified. The collector efficiency of the PTCS can be in the range of 40%–60%. It was also found that there existed a specified delay for the temperature of the HTF to response to the solar flux, which played a significant role in designing the PTCS. The heat loss effect on collector efficiency was also studied, which was about 220 W/m for the receiver with a 180°C temperature difference between the collector temperature and the ambient temperature, amounting to about 10% of the total solar energy incident on the collector. The encouraging results can provide fundamental data for developing the parabolic trough solar thermal power plant in China.

solar energy, parabolic trough solar collector, collector efficiency, lag behind, heat loss

Citation: Liu Q B, Wang Y L, Gao Z C, et al. Experimental investigation on a parabolic trough solar collector for thermal power generation. Sci China Tech Sci,

1 Introduction

Parabolic trough solar thermal power technology has obtained wide popularity in the three solar thermal power technologies [1]. Large scale parabolic trough collectors can supply the thermal energy that can be used to produce steam for a Rankine steam turbine generator. The PTCS is frequently employed for steam generation due to its high collector's efficiency at the middle temperatures (around 300°C) [2, 3]. The performance of the PTCS plays an important role in the parabolic trough solar power plant, which directly determines the investment cost. Many investigations on optimizing and improving the performance of the PTCS have been carried out [4–8].

Since the resource of solar energy is abundant in China, especially in the west, such as Qinghai Province, Tibet, Xinjiang Autonomous Regions, the parabolic trough solar thermal power technology has received extensive attention recently.

The main motive of this paper is to develop an experimental platform of the PTCS, and evaluate the performance of the PTCS. Furthermore, some key parameters that influence the performance of the PTCS, such as the solar flux, the flow rate of the HTF, heat loss, are also investigated. The encouraging results have been obtained, which can provide fundamental data for developing the parabolic trough solar thermal power plant in China.

2 Experiment platform and procedure

In order to investigate the PTCS for solar thermal power generation, an experiment platform was developed. The experiment platform mainly consists of four parts: the solar collectors, the heat transfer fluid (HTF) circulation, the cooling water circulation, and the measurement system.

The flow diagram of the experimental platform using synthetic oil as the circulate HTF is shown in Figure 1. The

HTF not only can circulate between the oil tank and the electric heater tank, but also can flow through the solar receiver unit. During a typical experiment, the HTF was firstly fed into the electric heater tank by a pump, and heated to a certain temperature. Then the HTF was pumped to the solar receiver unit to absorb the solar energy. The heated HTF leaving the receiver was cooled by the cooling water in a heat exchanger, and finally flowed back to the oil tank, the loop being finished. Considering the coefficient of volume expansion of the HTF at a high temperature, an expansion tank was fixed on the top of the experimental platform. It is worth noting that the energy provided by the electric heater is not considered in the process of evaluating the solar energy.

The main parameters of the PTCS are shown in Table 1.

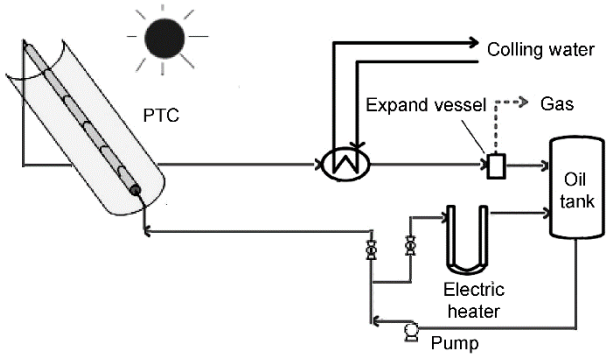

Figure 1 Schematic diagram of the experiment platform.

The single-axis-tracking PTCS was positioned in an east-west direction, and was composed of metal frame, silver-plated glasses mirrors, the collector receiver, and the collector's position controller. The position of the collector platform could be moved automatically and manually.

A diagram of the heat collector element (HCE) is shown in Figure 3. A solar receiver is a stainless steel tube with cermet selective coatings spread on the outside surface. In order to reduce the heat loss, the annulus space between the receiver and the glass envelope keeps the vacuum state. Both the ends of the HCEs are jointed bellows.

The temperatures were measured using temperature sensors of PT100 with the accuracy rating ±0.15°C inserted in the solar receiver as shown in Figure 3. The outside wall temperature of the receivers was also measured by temperature sensors of PT100. The direct normal irradiation was measured using a normal incidence pyrheliometer, and its precision can be controlled within 2%. The flow rate of the HTF in the loop was measured using a metal rotermeter, and its precision is in the range of 1%. The wind velocity was measured using the anemometer. All temperature and the direct normal irradiation data were automatically collected by the data acquisition system from Agilent Technologies. The solar thermal energy absorbed by the HTF can be computed by

$$Q_{\text{eff}} = \rho V C_p (T_0 - T_{\text{i}}). \quad (1)$$

The solar collector efficiency can be calculated by

$$\eta_{\text{c}} = Q_{\text{eff}} / IA, \quad (2)$$

where T_{i} and T_{o} stand for the inlet temperature and outlet temperature of the PTCS, respectively; V indicates the oil volume flow rate; ρ represents the density of the HTF; C_p is the isobaric specific heat capacity; I stands for the solar flux; A is the effective area of the parabolic trough concentrators. The heat loss in the parabolic trough field includes the heat loss from the receivers Q_{r}, Q_{c}, and the heat loss through the bellows and supporters Q_b.

The heat loss from receivers mainly includes two parts, one is the heat loss Q_{c} from the PTCS to the surroundings by convection, the other is the heat loss Q_{r} from the PTCS to the sky by radiation. The heat loss Q_{c} and Q_{r} can be obtained by the followings, respectively.

$$Q_{\text{c}} = h\pi D(T_{\text{g}} - T_{\text{a}}), \quad (3)$$

$$Q_{\text{r}} = \sigma\pi D\varepsilon(T_{\text{g}}^4 - T_{\text{sky}}^4), \quad (4)$$

where ε is the emissivity of the glass envelope outer surface; h stands for convection heat transfer coefficient; D is outer diameter of the receiver; σ indicates Stefan-Boltzmann constant; T_{g} and T_{sky} represent the temperature of the outside wall of the receivers and sky. The heat loss Q_{b} through the bellows can be estimated based on the ref. [9]. Detail report on the numerical simulation method for collector performance can be found in our previous work Correlations for the density ρ, thermal conductivity λ, isobaric specific heat capacity C_p and dynamic viscosity μ of the HTF named YD-300 can be described as follows:

$$\rho = 2.5714\times10^{-4}T^2 - 8.9333\times10^{-1}T + 1.2438\times10^{3} \ (\text{kg/m}^3);$$

$$\lambda = 7.4714\times10^{-8}T^2 - 1.3338\times10^{-4}T + 1.5580\times10^{-1} \ (\text{W/(m K)});$$

$$C_p = -1.1954\times10^{-3}T^2 + 4.6099T + 5.1196\times10^{2} \ (\text{kJ/(kg K)});$$

$$\mu = 9.7755\times10^{-8}T^4 - 1.9000\times10^{-4}T^3 + 1.3815\times10^{-1}T^2 - 4.4610\times10^{1}T + 5.4188\times10^{3} \ (\mu\text{Pa s}).$$

3 Results and discussion

Many important factors, such as the solar flux, the flow rate of the HTF and the heat loss, influence the performance of the PTCS for thermal power generation. Therefore, they are taken into account in this study as follows.

A typical result obtained in September 21, 2009 is shown in Table 2, in which the volume flow rate of the HTF is 0.45 m^3/s. T_{a}, T_{i}, T_{o} and η_{c} stand for the ambient temperature, the inlet temperature of HTF, outlet temperature of the HTF and collector efficiency, respectively.

Figure 4 shows the relationship between the efficiency of the PTCS and the solar flux under different volume flow rates. The simulation result has been also obtained considering the solar flux varying from 200 to 900 W/m^2 in accordance with the experimental condition. The flow rates of the HTF were fixed at 0.45 m^3/h, 0.28 m^3/h and 0.10 m^3/h, respectively. From Figure 4, it can be found that the collector efficiency was in a range of 40%–60%. The experimental data scattered the simulation line. Analyzing Figure 4, it can be found that the collector efficiency nonlinearly depends on the solar flux. When HTF flow rate was 0.45 m^3/h, the efficiency had an increase of 7% from 200 to 550 W/m^2, while only 3% from 550 to 900 W/m^2, and the maximum of collector efficiency could be obtained at the highest solar flux within the study range. A reason is that the mean temperature of the receiver increased drastically for these values, the heat gained by the HTF went up slowly due to the heat loss. It can be also seen from Figure 4 that the collector efficiency was very low at the flow rate of 0.10 m^3/h. Since the Reynolds number is below 1000, and the heat transfer between the receiver and the HTF becomes seriously worsened.

Table 2 Experiment data at a flow rate of 0.45 m^3/h

Time	T_a	T_i (°C)	T_o(°C)	I (W/m^2)	η_c
12:00	25.8	94.5	151.1	825	0.570
12:15	25.2	107.1	166.0	813	0.611
12:30	28.0	124.7	169.0	789	0.577
12:45	28.0	131.5	163.2	770	0.550
13:00	29.3	135.5	163.7	730	0.530
13:15	30.8	135.5	154.4	704	0.527
13:30	31.2	129.9	163.0	649	0.535
13:45	30.0	134.8	165.0	610	0.523
14:00	30.0	137.9	167.3	567	0.542
14:15	29.8	139.2	165.7	530	0.527
14:30	31.7	138.9	159.3	466	0.492

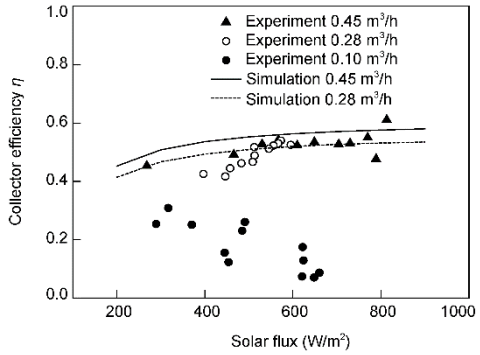

Figure 4 The variation of collector efficiency with solar flux.

Figure 5 shows the relationship between the collector efficiency and the solar flux from morning to afternoon. The experiment was carried out from 10:30 to 14:30, June 3, 2009. It was found that the collector efficiency in the afternoon was higher than in the morning. A possible reason is the heat capacity of the main structure of the PTCS, such as the metal brackets, bellows temperatures, were very low in the morning, and a larger percent of the solar thermal energy was absorbed by the body of the PTCS. With the decrease of the solar flux, the temperature of the HTF would not fall immediately due to high temperature of the main body structure of the PTCS. Therefore, the temperature response lagged behind the decrease of the solar flux. When the solar flux is variable, identifying the time interval of the temperature lag is essential.

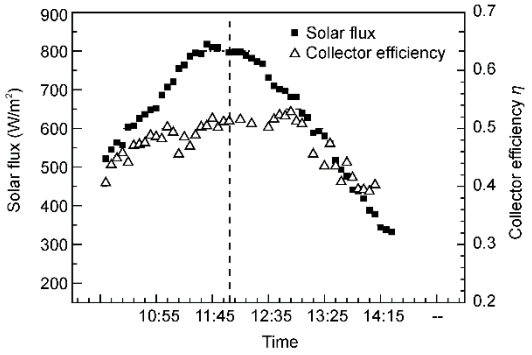

Figure 5 Variation of collector efficiency with solar flux.

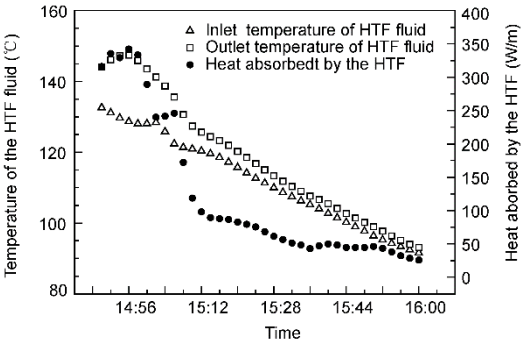

Figure 6 Variations of temperature of the HTF and heat absorbed by the HTF without sun.

The simplest case available for verifying the influence of the heat capacity is the case with no-sun on the absorber, as shown in Figure 6. The experiment was done from 14:50 to 16:00 in the afternoon, and the flow rate of the HTF was 0.40 m^3/h. It can be seen that the temperature difference between the outlet and inlet of the HTF still kept positive and became smaller with the time. This was because that the energy absorbed by the HTF was from the PTCS, such as receivers, bellows and supports. 15 min later, nearly at 15:05, the inlet and outlet temperatures tended to the same. This characteristic plays an important role in the design and operation of the parabolic trough solar power plants. The similar property was also reported by Senthilkumar et al. [11].

The thermal output of the PTCS depends on the energy that the absorbed solar radiation incident on the collector reduced the losses of the collector, including the heat loss, optical loss. So it is a key issue how to determine the heat loss. If the outside wall temperatures of the receivers are obtained, the heat loss in the parabolic trough field from the receivers Q_r can be easily calculated approximately for a known wind speed and ambient temperature. The method cannot depend on the receiver condition, such as vacuum, air, lost vacuum. In this paper, temperature sensors of PT100 were surrounded the receivers, and aluminum foils were used to prevent the temperature sensors from directly absorbing the normal irradiation. The similar measure method was performed by Liipfert et al. [12], who used an infrared camera to evaluate the in-situ thermal performance of parabolic trough receivers.

Figure 7 shows the heat loss and temperature difference of the HTF temperature above the ambient temperature with time. The experiment was done under the condition of the velocity of about 2 m/s and the ambient temperature in the range of 29.5–31.5°C. It can be found that the HTF temperature above the ambient temperature decreased with the time. It is mainly because the solar irradiation incident on the collector goes down with the time. It is noteworthy that the HTF temperature above the ambient temperature has a small decrease from 13:30 to 13:50. A possible reason is the effect of the shading of the collector supports and a little increase of solar irradiation.

As also seen from Figure 7, the heat loss by convection and radiation both decreased with the time, and the heat loss were about 220 W/m for the PTCS for a 180°C temperature difference between the collector temperature and the ambient temperature, which could amount to about 10% of the total solar energy incident on the collector.

4 Conclusion

In this paper an experiment platform of a parabolic trough solar collector system (PTCS) was developed for thermal power generation, and the performance of the parabolic trough solar collector was experimentally investigated with synthetic oil as the circulate heat transfer fluid (HTF). The collector efficiency of the PTCS can be obtained in the range of 40%–60%. It was also found that there exists a specified delay between the temperature response of the HTF and the solar flux, which played a significant role in designing the PTCS. The heat loss effect on collector efficiency was also studied, which was about 220 W/m for the receiver at a 180°C temperature difference between the collector temperature and the ambient temperature, amounting to about 10% of the total solar energy incident on the collector. The encouraging results can provide fundamental data for developing the parabolic trough solar thermal power plant in China.

Acknowledgement

This work was supported by the National Natural Science Foundation of China (Grant No. ……) and the National Basic Research Program of China ("973" Program) (Grant No. ……).

1 Price H, Lupfert E, Kearney D, et al. Advances in parabolic trough solar technology. J Sol Energ-T ASME, 2002, 124(2): 109–125
2 Kalogirou S, Lloyd S, Ward J. Modeling, optimization and performance evaluation of a parabolic trough solar collector steam generation system. Sol Energy, 1997, 60(1): 49–59
3 Bakos G C, Ioannidis I, Tsagas N F, et al. Design, optimization and conversion-efficiency determination of a line-focus parabolic-trough solar-collector (PTC). Appl Energ, 2001, 68(1): 43–50
4 Dudley V, Kolb G, Sloan M. Test Results: SEGS LS2 Solar Collector. Report of Sandia National Laboratories, SANDIA 94-1884. 1994
5 Quaschning V, Kistner R, Ortmanns W. Influence of direct normal irradiance variation on the optimal parabolic trough field size: A problem solved with technical and economical simulations. J Sol Energ-T ASME, 2002, 124(2): 160–164
6 Liipfert E, Pottler K, Ulmer S, et al. Parabolic trough optical performance analysis techniques. J Sol Energ-T ASME, 2007, 147(2): 147–152
7 Yang Y P, Cui Y H, Hou H J, et al. Research on solar aided coal-fired power generation system and performance analysis. Sci China Tech Sci, 2008, 51(8): 1211–1221
8 Jin H G, Hong H, Sui J, et al. Fundamental study of novel mid-and low-temperature solar thermochemical energy conversion. Sci China Tech Sci. 2009, 52(5): 1135–1152
9 Odeh S D, Morrison G L, Behnia M. Modeling of parabolic trough direct steam generation solar collectors. Sol Energy, 1998, 62(6): 395–406
10 Gao Z C, Sui J, Liu Q B, et al. Modeling and analysis of 30 m^2 parabolic trough collector (in Chinese). In: Chinese Society of Engineering Thermophysics Conference. Beijing: Chinese Society of Engineering Thermophysics, 2009
11 Senthilkumar S, Perumal K, Srinivasan P S S. Optical and thermal performance of a three-dimensional compound parabolic concentrator for spherical absorber. Sadhana-Acad P Eng S, 2009, 34(3): 369–380
12 Liipfert E, Riffelmann K J, Price H. Experimental analysis of overall thermal properties of parabolic trough receivers. J Sol Energ-T ASME, 2008, 130(2): 021007